J Physiol 586.21 (2008) pp 5203–5214

The Journal of Physiology

Transmural variation in myosin heavy chain isoform expression modulates the timing of myocardial force generation in porcine left ventricle

Julian E. Stelzer, Holly S. Norman, Peter P. Chen, Jitandrakumar R. Patel and Richard L. Moss

Department of Physiology, University of Wisconsin School of Medicine and Public Health, Madison, WI 53706, USA

Recent studies have shown that the sequence and timing of mechanical activation of myocardium vary across the ventricular wall. However, the contributions of variable expression of myofilament protein isoforms in mediating the timing of myocardial activation in ventricular systole are not well understood. To assess the functional consequences of transmural differences in myofilament protein expression, we studied the dynamic mechanical properties of multicellular skinned preparations isolated from the sub-endocardial and sub-epicardial regions of the porcine ventricular midwall. Compared to endocardial fibres, epicardial fibres exhibited significantly faster rates of stretch activation and force redevelopment (k_{tr}), although the amount of force produced at a given [Ca^{2+}] was not significantly different. Consistent with these results, SDS-PAGE analysis revealed significantly elevated expression of α myosin heavy chain (MHC) isoform in epicardial fibres (13 ± 1%) *versus* endocardial fibres (3 ± 1%). Linear regression analysis revealed that the apparent rates of delayed force development and force decay following stretch correlated with MHC isoform expression ($r^2 = 0.80$ and $r^2 = 0.73$, respectively, $P < 0.05$). No differences in the relative abundance or phosphorylation status of other myofilament proteins were detected. These data show that transmural differences in MHC isoform expression contribute to regional differences in dynamic mechanical function of porcine left ventricles, which in turn modulate the timing of force generation across the ventricular wall and work production during systole.

(Received 23 July 2008; accepted after revision 11 September 2008; first published online 11 September 2008)
Corresponding author J. E. Stelzer: Department of Physiology, University of Wisconsin School of Medicine and Public Health, 601 Science Drive, Madison, WI 53711, USA. Email: stelzer@physiology.wisc.edu

The human heart is an extremely robust organ that is capable of beating nearly 100 000 times daily over the human lifespan. Despite operating as a single contractile unit to power ejection, however, the left ventricle exhibits extensive electrical and mechanical heterogeneity, i.e. the pattern of ventricular activation and the timing and extent of muscle contraction and lengthening in the human heart varies on a regional basis (Bogaert & Rademakers, 2001). Thus, efficient cardiac function requires precise coordination of electrical activation and myocardial contraction (Markhasin *et al.* 2003), the importance of which is underscored by the observation that disruptions in the pattern of ventricular electro-mechanical activation have been implicated in the development of cardiac dysfunction in congestive heart failure (Kass *et al.* 1999; Nelson *et al.* 2000; Cazeau *et al.* 2001; Sengupta *et al.* 2005, 2006). The mechanisms underlying the coordination of mechanical function across the ventricular wall during systolic ejection remain unclear.

Recent studies have shown that myocardial shortening in the endocardium precedes the shortening of epicardial fibres during isovolumic contraction (Ashikaga *et al.* 2004; Sengupta *et al.* 2005; Buckberg *et al.* 2006), a phenomenon that results from the sequential activation of myocardium radially towards the epicardium following the initial depolarization of the endocardium. Despite this transmural delay in electrical activation, it has been observed that endocardial and epicardial fibres shorten synchronously during systolic ejection in the normal heart (Ashikaga *et al.* 2004, 2007; Buckberg *et al.* 2006). This suggests that the mechanical properties of the endocardium and epicardium are functionally distinct in order to maintain an appropriate level of force generation and work production across the ventricular wall. To date, however, most studies have focused on the regional differences in the electrical properties of ventricular myocytes (Liu *et al.* 1993; Laurita *et al.* 2003) while relatively little is known about regional diversity in mechanical properties.

©2008 The Authors. Journal compilation © 2008 The Physiological Society

DOI: 10.1113/jphysiol.2008.160390

At the myofilament level, the speed and force of myocardial contraction during systolic ejection are largely determined by the inherent enzymatic and mechanical properties of myosin heavy chain (MHC) isoforms and the relative abundance of their expression. In mammals, two distinct cardiac isoforms have been identified, α and β (Hoh *et al.* 1979), of which the β MHC isoform displays significantly slower actin-activated ATPase activity, shortening velocity, and cross-bridge cycling kinetics (reviewed by Schiaffino & Reggiani, 1996). In adult human ventricles, the faster α MHC isoform is believed to comprise less than 10% of the total ventricular MHC composition (Miyata *et al.* 2000). The functional importance of such a low abundance of α MHC expression is unclear, although several studies have demonstrated that the expression of α MHC is dramatically down-regulated under conditions of chronic congestive heart failure (Lowes *et al.* 1997; Miyata *et al.* 2000; Reiser *et al.* 2001). This raises the possibility that even small scale shifts in the expression of α MHC can have significant effects on contractile function, especially if low abundance MHC isoforms are localized to specific regions of the heart.

In this regard, it has been shown that the expression of α MHC in mammalian hearts is more abundant in the epicardium than in the endocardium in the left ventricular midwall (Litten *et al.* 1985; Kuro-o *et al.* 1986; Bouvagnet *et al.* 1989; Bougaisky *et al.* 1990; Reiser *et al.* 2001; Carnes *et al.* 2004). Despite the gradient in α MHC, however, the functional consequences of this pattern of MHC isoform expression in global heart function have yet to be established. Intriguingly, it has been recently hypothesized that higher expression of the α MHC isoform could account for the faster time course of unloaded cell shortening in epicardial cells compared with endocardial cells isolated from canine left ventricles, because variability in Ca^{2+} handling kinetics in epicardial and endocardial cells alone was not sufficient to explain these differences (Cordeiro *et al.* 2004). Furthermore, a computational model by Campbell *et al.* (2008) to quantitatively test the hypothesis of Cordeiro *et al.* (2004) found that an acceleration in cross-bridge kinetics, as would be expected with higher α MHC isoform expression in epicardial cells, could reproduce the faster time courses of unloaded shortening reported by Cordeiro *et al.* (2004). Taken together, these studies suggest that transmural differences in MHC isoform expression in the mammalian ventricle could have a profound impact on cardiac contractile function; therefore this study was undertaken to examine the functional effects of variable MHC isoform expression across the ventricular midwall. Here we show that transmural differences in MHC isoform expression contribute to regional differences in dynamic mechanical function of porcine left ventricles, which in turn modulates the timing of force generation and work production across the ventricular wall.

Methods

Ethical approval

All animal procedures were approved by the Institutional Animal Care and Use Committees and were conducted in accordance with the Guiding Principles in the Care and Use of Animals, as approved by the Council of the American Physiological Society.

Experimental animals

Adolescent pigs ($n = 5$) of either sex and weighing 45 ± 3 kg were employed in this study. Following initial sedation with a combination of ketamine (1 g), atropine (0.8 mg) and acepromazine (30 mg) given intramuscularly, an intravenous catheter was inserted in the superficial ear vein of the pigs and thiopental sodium (250 mg), and α-chloralose (1.5 g) were infused as previously described (McDonald *et al.* 1995). The animals were artificially ventilated with supplemental oxygen, and arterial levels of pH, O_2 and P_{CO_2} were continuously monitored to ensure maintenance of physiological oxygenation and acid–base balance. The heart was exposed by bilateral thoracotomy with trans-sternotomy and the mid free-wall was excised and immediately frozen in liquid nitrogen. The animals were killed by removal of the heart. Anaesthesia, surgery and general care of the animals strictly conformed to institutional guidelines and were reviewed and approved by the University of Wisconsin Medical School Animal Care and Use Committee.

Apparatus and experimental protocols

Solution compositions for mechanical experiments were calculated using a computer program (Fabiato, 1988) and known stability constants (Godt & Lindley, 1982) corrected to pH 7.0 and 22°C. All solutions contained (mM): 100 *N*,*N*-bis(2 hydroxy-ethyl)-2-aminoethanesulphonic acid (Bes), 15 creatine phosphate, 5 dithiothreitol, 1 free Mg^{2+} and 4 MgATP; pCa 9.0 solution contained 7 EGTA and 0.02 $CaCl_2$; pCa 4.5 contained 7 EGTA and 7.01 $CaCl_2$; and pre-activating solution contained 0.07 EGTA. Ionic strength of all solutions was adjusted to 180 mM with potassium propionate. Solutions containing different $[Ca^{2+}]_{free}$ were prepared by mixing appropriate volumes of solutions of pCa 9.0 and pCa 4.5.

On the day of the experiment, a small piece of tissue (1 cm × 1 cm × 1 cm, approximately 10% depth) from the sub-endocardial or sub-epicardial layers of the mid free-wall was isolated for preparation of skinned myocardium for mechanical experiments (Stelzer *et al.* 2006*a*). Skinned myocardium was prepared by mechanically

©2008 The Authors. Journal compilation © 2008 The Physiological Society

disrupting the ventricular tissue for ∼2 s using a Polytron (Kinematica) (Stelzer *et al.* 2006*a*), which yielded multicellular preparations of 100–250 μm in width and 600–900 μm in length. The myocardial preparations were then skinned in a solution containing Triton X-100 for 30 min, and then the ends of the preparations were attached to the arms of a position motor and force transducer as previously described (Stelzer *et al.* 2006*a*). Motor position and force signals were sampled using SL Control software (Campbell & Moss, 2003) and saved to computer files for later analysis.

Force–pCa relationships

Methods for obtaining and analysis of force–pCa relationships are described in detail elsewhere (Stelzer *et al.* 2006*a*). Briefly, each myocardial preparation was allowed to develop steady force in solutions of varying $[Ca^{2+}]_{free}$. The difference between steady-state force and the force baseline obtained following the 20% slack step was measured as the total force at that $[Ca^{2+}]_{free}$. Active force was then calculated by subtracting Ca^{2+}-independent force in solution of pCa 9.0 from the total force and was normalized to the cross-sectional area of the preparation, which was calculated from the width of the preparations assuming a cylindrical cross-section. Force–pCa relationships were constructed by expressing sub-maximal force (P) at each pCa as a fraction of maximal force (P_o) determined at pCa 4.5, i.e. P/P_o. The apparent cooperativity in the activation of force development was inferred from the steepness of the force–pCa relationship and was quantified using a Hill plot transformation of the force–pCa data (Stelzer *et al.* 2006*a*). The force–pCa data were fitted using the equation $P/P_o = [Ca^{2+}]^n/(k^n + [Ca^{2+}]^n)$, where n is the Hill coefficient, and k is the $[Ca^{2+}]$ required for half-maximal activation (i.e. pCa_{50}).

Rate of force redevelopment

The rate constant of force redevelopment (k_{tr}) in skinned myocardium was assessed as previously described (Fitzsimons *et al.* 2001). Each skinned preparation was transferred from relaxing to an activating solution of pCa 4.5 and allowed to generate steady-state force. The myocardial preparation was rapidly (< 2 ms) slackened by 20% of its original length, resulting in a rapid reduction of force to near zero, i.e. < 5% of steady isometric force. This was followed by a brief period of unloaded shortening (10 ms) after which the preparation was rapidly restretched to its original length. The apparent rate constant of force redevelopment (k_{tr}) was estimated by linear transformation of the half-time of force redevelopment, i.e. $k_{tr} = 0.693/t_{1/2}$, as previously described (Fitzsimons *et al.* 2001).

Stretch activation experiments

For stretch activation experiments, fibre length in relaxing solution was adjusted to achieve a sarcomere length of ∼2.1 μm for measurement of initial isometric force and for subsequent imposition of stretch. To evoke stretch activation a rapid stretch (∼10 muscle lengths s^{-1}) of 1% of muscle length (Stelzer *et al.* 2006*b*) was imposed on fibres that were activated to develop maximal force (P_o). The method used for measuring the stretch activation variables have been described in detail previously (Stelzer *et al.* 2006*b*). The amplitudes of the phases of the stretch activation responses were measured as follows and are shown in Fig. 2:

P_1, measured from pre-stretch steady-state force to the peak of phase 1,

P_2, measured from pre-stretch steady-state force to the minimum force value at the end of phase 2,

P_3, measured from pre-stretch steady-state force to the peak value of delayed force, and

P_{df}, difference between P_3 and P_2.

All amplitudes were normalized to the pre-stretch Ca^{2+} activated force to allow comparisons between preparations which generated different absolute isometric force. The apparent rate constants were estimated for phase 2 (k_{rel}, s^{-1}) between the peak of phase 1 and the minimum of phase 2 and for phase 3 (k_{df}, s^{-1}) from the beginning of force redevelopment following phase 2 to the completion of delayed force development, and are reported by linear transformation of the half-time of relaxation of force (k_{rel}) or delayed force development (k_{df}) (i.e. k_{rel} or $k_{df} = 0.693/t_{1/2}$).

Determination of myosin heavy chain isoform content

At the conclusion of each experiment, cardiac preparations were cut free, placed in a microcentrifuge tube containing 10 μl of SDS–urea–thiourea sample buffer (50 mM Tris, 75 mM dithiothreitol, 8 M urea, 2 M thiourea, 30% glycerol, 3% SDS and 0.01% Bromophenol Blue, pH 6.8) and stored at −80°C. For analysis of MHC protein content by SDS-PAGE, microcentrifuge tubes were first sonicated for 15 min and centrifuged to collect any un-dissolved particulate matter. Sample buffer (3–6 μl) containing myofibrillar proteins was then loaded on to large format (18 cm × 16 cm) polyacrylamide gels. MHC isoform content was assessed using acrylamide gels cross-linked with N-N′ diallyltartardiamide (DATD) (Warren & Greaser, 2003). Stacking gels contained 3%

©2008 The Authors. Journal compilation © 2008 The Physiological Society

total monomer/15% DATD co-monomer, 10% glycerol, 130 mM Tris (pH 6.8) and 0.1% SDS. Separating gels contained 6% total monomer/2.6% DATD co-monomer, 10% glycerol, 0.37 M Tris (pH 8.8) and 0.1% SDS. Gels were run using a Hoefer SE 600 Vertical Electrophoresis Unit with 0.75 mm spacers and a Bio-Rad PowerPac 300 power supply. The running buffer consisted of 25 mM Tris (base), 192 mM glycine and 0.1% SDS, pH 8.3. The gels were run at 16 mA for 10 h at 4°C and then visualized by silver staining (Schevchenko *et al.* 1996). The relative proportions of α and β MHC isoforms were determined by densitometric analysis of silver-stained gels using LaserPix software (Bio-Rad Laboratories) as previously described (Stelzer *et al.* 2007). This method reproducibly detects 2 ng of protein per band and has linearity of stain between 2 and 70 ng of protein per band. Linearity of staining was assured by running samples in parallel lanes following several serial dilutions. Our densitometric analysis of MHC isoform bands revealed that the α MHC band can be consistently detected when its staining intensity was approximately 1% that of the β MHC band.

Determination of myofibrillar protein phosphorylation

Myofibrillar proteins of porcine myocardium were separated by SDS-PAGE using 10–14.5% Tris-HCl criterion gradient precast gel (Bio-Rad). To detect phosphorylated proteins, the gels were stained with Pro-Q Diamond following the protocol of the vendor (Molecular Probes) as previously described (Stelzer *et al.* 2006*c*). Briefly, the gels were (a) fixed in 10% glacial acetic acid–50% methanol (1.5 h; 3 solution changes), (b) washed with dH_2O (1 h; 6 solution changes), (c) stained with Pro-Q Diamond (1.5 h), and (d) destained with Pro-Q Diamond destaining solution (Molecular Probes) overnight. To detect myofibrillar proteins, the gels were stained with SYPRO Ruby (Molecular Probes; 3 h) and destained with 7% glacial acetic acid–10% methanol (2 h; 4 solution changes). Gels of phosphoprotein and total myofibrillar proteins were scanned using a UVP BioImaging System and quantified using LaserPix. The skinned myocardial preparations loaded on the gels were prepared from a total of four porcine hearts. To quantify protein phosphorylation levels, different volumes (in the range of 3–6 μl) of samples prepared from sub-endocardial and sub-epicardial myocardium were loaded on the same gel. After gel electrophoresis, the gels were stained with SYPRO Ruby to detect proteins and with Pro-Q Diamond to detect phosphoproteins and the area and mean raw optical density of protein and phosphoprotein bands were determined using LabWorks analysis software (UVP BioImaging System, CA, USA). The product of the area and mean raw optical density *versus* volume loaded were generated and a first order linear regression was fitted to the data points to determine the slope of the relationship between optical density and volume loaded as previously described (Stelzer *et al.* 2006*c*).

Determination of light chain phosphorylation levels was also performed by two-dimensional gel electrophoresis in a mini gel system as previously described (Stelzer *et al.* 2006*d*). Briefly, the first dimensional iso-electric focusing (IEF) tube gels containing 8 mM urea, 4% acrylamide–bisacrylamide (30% acrylamide–bisacrylamide solution, Bio-Rad), 2% Triton X-100, 2% ampholyte (pH 4.1–5.9; Biorad), 0.02% ammonium persulphate and 0.2% TEMED were pre-focused first at 200 V for 15 min and then at 400 V for 15 min. The samples were then loaded on to the gels and electrofocused first at 500 V for 20 min and then at the 750 V for 4 h 40 min. The IEF tube gels were ejected on to a 12.5% Tris-HCl criterion precast gel (Bio-Rad) and electrophoresed at 150 V for 1 h 30 min. The gels were then silver stained at room temperature using published methods (Schevchenko *et al.* 1996) with minor modifications, as follows: the gels were: (a) incubated in fixing solution containing 50% methanol and 10% acetic acid for 20 min; (b) washed with distilled water for 20 min (4 solution changes); (c) incubated in 0.01% sodium thiosulphate solution for 1.5 min and then rinsed 4 times with distilled water; (d) incubated in 0.09% silver nitrate solution for 20 min and then rinsed 4 times with distilled water; (e) incubated in developing solution containing 0.0004% sodium thiosulphate, 2% potassium carbonate and 0.0068% fomaldehyde until proteins were visible and then rinsed 4 times with distilled water; and (f) incubated in destaining solution containing 10% methanol and 10% acetic acid for 20 min, rinsed 4 times in distilled water and finally rinsed (with slow rotation) overnight in distilled water. The gels were then dried between two sheets of cellophane overnight, and the per cent regulatory light chain (RLC) phosphorylation was quantified using UVP BioImaging System and LaserPix software.

Statistical analysis

Cross-sectional areas of skinned preparations were calculated by measuring the width of the mounted preparation and assuming a cylindrical cross-section. Sub-maximal Ca^{2+}-activated force (P) was expressed as a fraction of the force (P_o) generated at pCa 4.5, i.e. P/P_o. Comparisons of force–pCa relationships, apparent rate of force redevelopment, and stretch activation variables between groups were done using a one-way analysis of variance (ANOVA) or a Student's t test. Linear regression analysis was performed using Sigma Plot 8 software. All data are reported as means ± S.E.M. Significance level was set at $P < 0.05$.

©2008 The Authors. Journal compilation © 2008 The Physiological Society

Table 1. Steady state mechanical properties of porcine endocardial and epicardial fibres isolated from the left ventricular midwall

	α MHC content (% of total)	F_{min} (mN mm^{-2})	F_{max} (mN mm^{-2})	pCa_{50}	n_H
Sub-endocardium	2.8 ± 0.6	0.6 ± 0.3	23.3 ± 1.6	5.72 ± 0.01	4.35 ± 0.34
Sub-epicardium	12.5 ± 1.4*	0.7 ± 0.3	24.5 ± 1.8	5.73 ± 0.01	4.17 ± 0.37

Data are means $\pm$ S.E.M. from 19 endocardial and 19 epicardial fibres. MHC, myosin heavy chain, F_{max}, maximal Ca^{2+}-activated force at pCa 4.5; F_{min}, Ca^{2+}-independent force at pCa 9.0; pCa_{50}, pCa required for half-maximal force generation; n_H, Hill coefficient for total force–pCa relationship. *Significantly different from endocardium, $P < 0.05$.

Results

Steady-state mechanical properties of porcine skinned endocardial and epicardial myocardium

The steady-state mechanical properties of skinned myocardium isolated from the endocardial and epicardial regions of porcine ventricular midwalls are summarized in Table 1. As shown in Fig. 1, skinned preparations from the endocardium and epicardium exhibited similar force–pCa relationships, i.e. there were no differences in either the amount of force produced by cardiac preparations at maximal and sub-maximal activating [Ca^{2+}] or in the steepness of the force–pCa relationship (Hill coefficient, n_H). The lack of difference in steady-state mechanical properties of left ventricular myocardium is in agreement with previous studies of rat myocardium performed at similar sarcomere lengths (Diffee & Nagle, 2003; Cazorla *et al.* 2005).

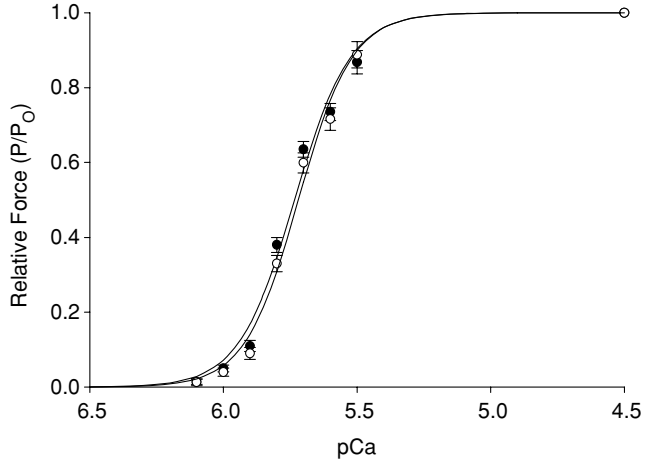

Figure 1. Force–pCa relationships of endocardial and epicardial myocardium
Myocardium isolated from epicardial (●) and endocardial left ventricular midwall (○) displayed similar force–pCa relationships. Data points are means $\pm$ S.E.M. of 19 endocardial and 19 epicardial fibres.

Transmural differences in the stretch activation response and kinetics of force redevelopment

The stretch activation response in porcine skinned myocardium was studied in endocardial and epicardial fibres by imposing a stretch of 1% of initial muscle length during maximal Ca^{2+} activation. To facilitate comparisons of stretch activation parameters, the phases of the stretch activation response were normalized to the isometric force preceding the application of stretch as indicated in Fig. 2, where P_2 is the minimum force at the end of phase 2, P_{df}, is the trough-to-peak excursion of force in phase 3, and P_3 is the amplitude of phase 3 measured from the pre-stretch isometric force. The amplitude of phase 1 (P_1) was not assessed in this work. The amplitude of the delayed force response (phase 3) is indicative of the

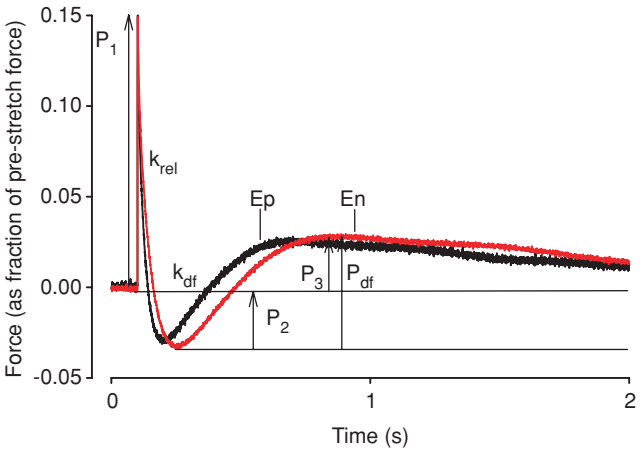

Figure 2. Stretch activation responses of porcine skinned myocardium isolated from the endocardial and epicardial midwall
Force transients following a stretch of 1% of muscle length were recorded at maximal [Ca^{2+}] activations in skinned fibres from the endocardium (En) and the epicardium (Ep). Once a steady-state isometric force was achieved at maximal Ca^{2+} activation, the muscle was stretched and then held at the longer length, as described in Methods. These representative transients are normalized to pre-stretch isometric force corresponding to the force base-line, which is arbitrarily set at zero. The recorded variables are labelled on the force record and described in the text.

©2008 The Authors. Journal compilation © 2008 The Physiological Society

Table 2. Stretch activation variables and rates of force redevelopment in skinned endocardial and epicardial myocardium

	P_2 (P/P_o)	P_3 (P/P_o)	P_{df} (P/P_o)	k_{rel} (s^{-1})	k_{df} (s^{-1})	k_{tr} (s^{-1})
Sub-endocardium	-0.040 ± 0.004	0.031 ± 0.003	0.071 ± 0.004	21.74 ± 1.32	2.44 ± 0.12	2.57 ± 0.17
Sub-epicardium	-0.037 ± 0.005	0.030 ± 0.004	0.067 ± 0.005	26.31 ± 1.45*	2.99 ± 0.13*	3.13 ± 0.19*

Data are reported as means ± S.E.M. from 19 endocardial and 19 epicardial preparations activated at maximal [Ca^{2+}] (pCa 4.5). The myosin heavy chain isoform distribution of fibres is the same as reported in Table 1. Stretch activation amplitudes and apparent rate constants data were obtained from force transients in response to stretches of 1% of muscle length and the apparent rate constant of force redevelopment (k_{tr}) was obtained by performing the slack–restretch manoeuver. Stretch activation amplitude variables are presented as a fraction of pre-stretch isometric force (P_o). Apparent rate constants for k_{df}, k_{rel} and k_{tr} were estimated by a linear transformation of the half-time of each variable as described in the Methods. *Significantly different from endocardium, $P < 0.05$.

number of cross-bridges recruited by stretch (Stelzer *et al.* 2006*b*). No differences in P_3 were found between endocardial and epicardial fibres (Table 2), suggesting that the number of cross-bridges recruited by stretch is similar and independent of expression of MHC isoforms. The minimum amplitude following rapid force decay (P_2) dipped below the isometric force baseline in all fibres and is therefore reported as a negative value (Table 2). No significant differences in P_2 were detected between endocardial and epicardial fibres. Consequently, P_{df}, which is the overall trough-to-peak amplitude of phase 3, was also similar (Table 2).

In contrast to the lack of differences observed in the amplitudes of stretch activation, significant differences in the apparent rates of force decay (k_{rel}) and delayed force development (k_{df}) were observed in endocardial and epicardial myocardium (Table 2). As shown in the records of Fig. 2, the overall rate of stretch activation is slowed in endocardial fibres, with peak delayed force occurring significantly later. In addition, endocardial fibres displayed k_{rel} values that were approximately 80% of those in epicardial fibres (Table 2), indicating a decrease in the apparent rate of cross-bridge detachment. Endocardial fibres also exhibited k_{df} values that were significantly slower than epicardial fibres (Table 2), suggesting that the cooperative recruitment of cross-bridges into strongly bound states was also protracted.

To complement the measurement of stretch activation, we also investigated the effects of variable MHC isoform expression on the kinetics of force redevelopment (k_{tr}) by subjecting endocardial and epicardial fibres to a modified stretch–release protocol at maximal Ca^{2+} activations (Brenner & Eisenberg, 1986). Regional differences in k_{tr} mirrored differences in stretch activation kinetics such that endocardial fibres exhibited k_{tr} values that were significantly slower than epicardial fibres (Table 2). Since k_{tr} is thought to be the sum of the forward (f_{app}) and reverse (g_{app}) rate constants describing the transitions between force-generating and non-force-generating states (Brenner & Eisenberg, 1986), differences in k_{tr} can be attributed to changes in one or both rate constants. In this case, the slowing of k_{tr} in endocardial fibres is probably due to a decrease in both f_{app} and g_{app} because the stretch activation variables of k_{df} and k_{rel} were both decreased in endocardial fibres.

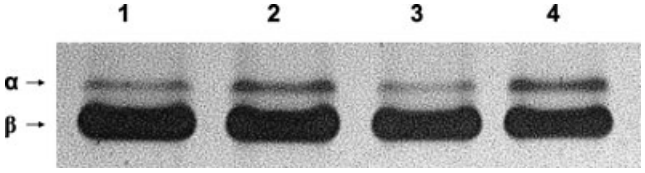

Figure 3. Regional variation in myosin heavy chain (MHC) composition in porcine ventricular myocardium
Myosin heavy chain (MHC) isoform content was determined using 6% SDS-PAGE. The relative proportions of α and β MHC isoforms were determined by densitometric analysis gels following a silver-staining protocol. In this representative gel it can be seen that muscle fibres isolated from the endocardial midwall (lane 1 and lane 3) expressed less cardiac α MHC (3.5% and 2.2% of the total MHC content, respectively) than muscle fibres isolated from the epicardial midwall (lane 2 and lane 4) of the left ventricle (14.1% and 13.7% of the total MHC content, respectively).

Myosin heavy chain isoform expression and myofilament protein phosphorylation in ventricular endocardial and epicardial myocardium

The composition of MHC isoforms was analysed for each skinned preparation used for mechanical experiments. Our results show that in the midwall region of the left ventricle, more α MHC is expressed in epicardial fibres *versus* endocardial fibres ($13 \pm 1\%$ and $3 \pm 1\%$, respectively) (Table 1). Figure 3 shows a representative SDS-PAGE gel demonstrating higher expression of α MHC in endocardial fibres isolated from the same left ventricle. Figure 4 is a scatter plot depicting the relationship between α MHC expression and the apparent rates of delayed force development (k_{df}) and force decay (k_{rel}) following stretch in individual fibres isolated from the endocardium and epicardium. It can be seen that when a regression line is fitted through the data, a significant correlation exists between α MHC expression and k_{df} ($r^2 = 0.80$,

©2008 The Authors. Journal compilation © 2008 The Physiological Society

$P < 0.05$) (Fig. 4*A*) and k_{rel} ($r^2 = 0.73$, $P < 0.05$) (Fig. 4*B*), suggesting that the accelerated stretch activation response in epicardial fibres is mostly due to higher expression of α MHC.

In contrast to MHC isoform expression, no significant differences in the relative abundance or phosphorylation status of other myofilament proteins in endocardial and epicardial preparations were detected (Fig. 5*A*). Figure 5*B* is an example of phosphoprotein analysis using SYPRO-Ruby and Pro-Q Diamond staining, which shows the expression levels and phosphorylation levels of cardiac myosin binding protein-C and troponin I (TnI) to be similar in the endocardium and epicardium. Figure 6 illustrates a representative two-dimensional gel used to determine the phosphorylation levels of myosin regulatory light chain in endocardial (left panel) and epicardial (right panel) fibres. Densitometric analysis of the spots revealed that RLC phosphorylation was not significantly different between endocardial and epicardial fibres.

Discussion

We examined the contractile properties of multicellular myocardial preparations isolated from the endocardial and epicardial midwall of porcine left ventricles. Our results showed that at maximal Ca^{2+} activations, the overall rate of stretch activation in epicardial fibres was significantly accelerated compared to endocardial fibres and was correlated with an increased expression of the faster α MHC isoform. Such differences in the kinetic response to fibre stretch across the ventricular wall would be expected to modulate the timing of fibre shortening during systolic ejection, and thereby, the rate of force generation and cardiac output. Thus, our data demonstrate that the regional distribution of MHC isoforms in the heart contributes to the heterogeneity in contractile function that underlies the modulation of the rate of force development and pressure generation *in vivo*.

Electromechanical coupling and myocyte function

Normal cardiac function requires that transmural differences in contractile function of individual myocytes be coupled to their respective calcium handling properties. Studies which have examined the differences in calcium handling properties across the left ventricular wall have found significant functional heterogeneity, with endocardial myocytes exhibiting significantly prolonged action potential duration (Liu *et al.* 1993) and a slower decay in the intracellular calcium transient compared with epicardial myocytes in canine ventricles, in part, due to a decreased expression of sarcoplasmic reticulum (SR) Ca^{2+}-ATPase (SERCA2a) (Laurita *et al.* 2003). Furthermore, endocardial myocytes exhibit reduced Ca^{2+} load in the SR compared with epicardial myocytes, which would contribute to the slower intracellular calcium transients and cell shortening kinetics observed in canine endocardial myocytes (Cordeiro *et al.* 2004). Taken together, these studies show that endocardial myocytes have significantly diminished SR function, which would be predicted to slow the cross-bridge cycling kinetics and rates of force development in contracting myocardium. Consistent with these results, our findings suggest that at the myofilament level, the overall rate of

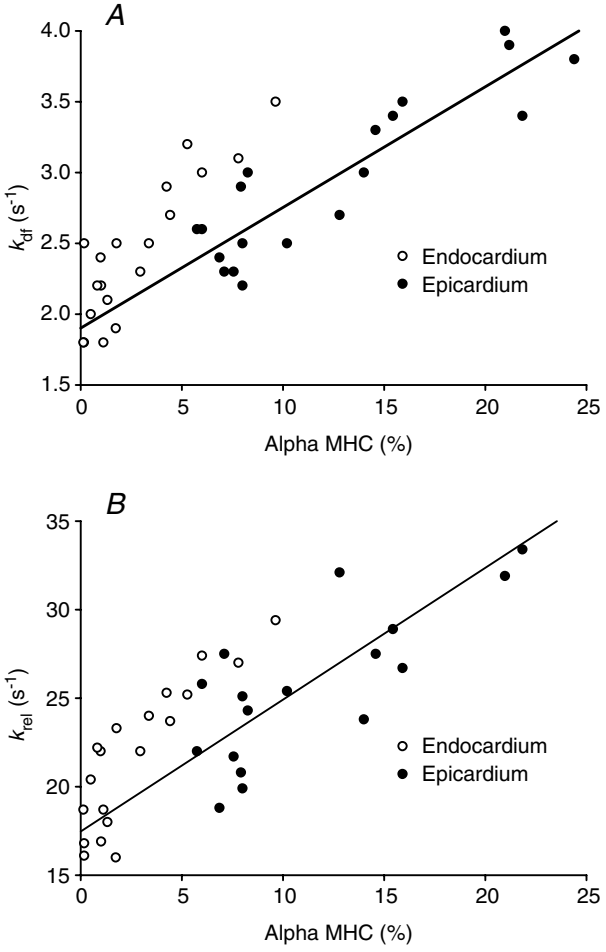

Figure 4. Linear regression analysis of α myosin heavy chain (MHC) expression and stretch activation kinetics
The relationship between expression of α MHC (as percentage of total MHC content) and the apparent rates of stretch-induced delayed force development (k_{df}) (*A*) and force decay (k_{rel}) (*B*) was determined by linear regression analysis in 19 endocardial (○) and 19 epicardial (●) fibres. A significant positive correlation was found between increased α MHC expression and accelerated k_{df} and k_{rel} in the endocardial and epicardial midwall of porcine left ventricle which is described by the regression equations: k_{df} (s^{-1}) = 0.085 (% α MHC) + 1.901 ($r^2 = 0.80$, $P < 0.05$), and k_{rel} (s^{-1}) = 0.745 (% α MHC) + 17.463 ($r^2 = 0.73$, $P < 0.05$).

©2008 The Authors. Journal compilation © 2008 The Physiological Society

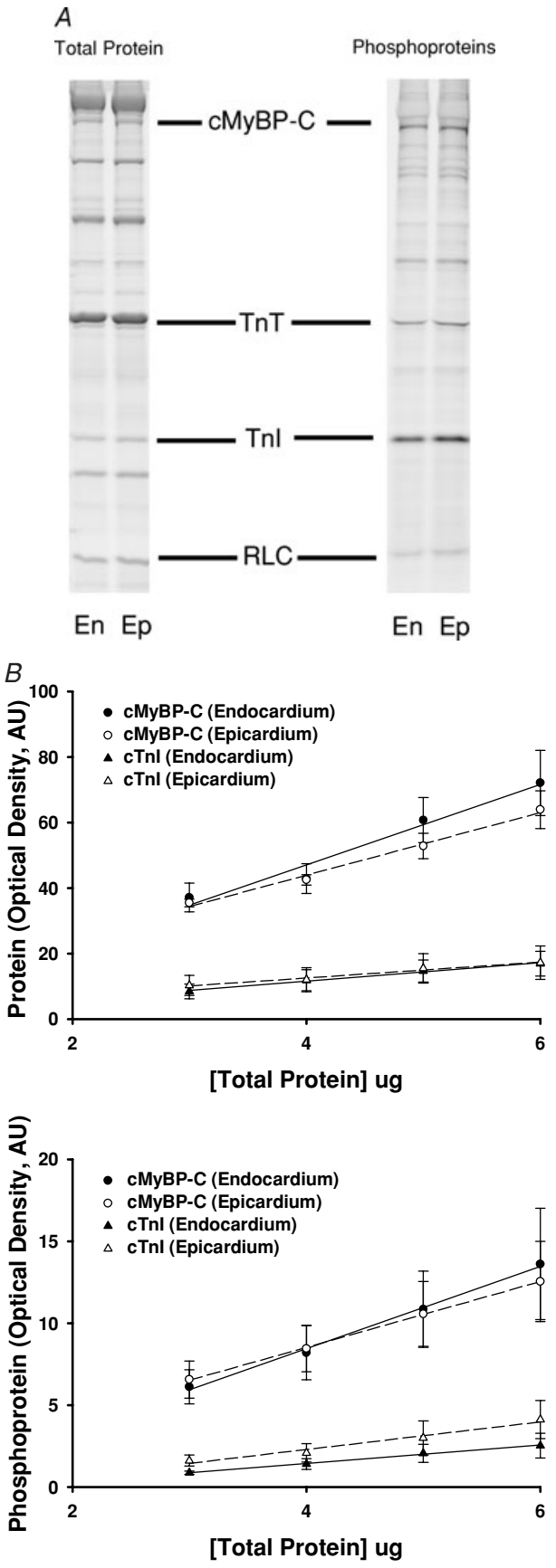

Figure 5. Determination of myofibrillar protein phosphorylation levels
A, representative SDS-PAGE (6 μg load) of the basal phosphorylation state of myofibrillar proteins in myocardium isolated from the endocardial (En) and epicardial (Ep) midwall. Preparation of porcine myocardial preparations loaded on the gel and analysis of phosphorylation status of proteins was performed as described in the Methods. SYPRO-Ruby stained gel for total proteins (left lanes) and Pro-Q Diamond-stained gel specific for phosphorylated proteins (right lanes). cMyBP-C, myosin binding protein-C; TnT, troponin T; TnI, troponin I; RLC, regulatory light chain. *B*, the slopes of protein and phosphoprotein determined from plots of area $\times$ mean raw optical density *versus* volume loaded for endocardial and epicardial myocardium. Different volumes of skinned endocardial and epicardial myocardial samples prepared from five porcine hearts were separated by SDS-PAGE and stained with SYPRO-Ruby for total proteins (top panel) and Pro-Q Diamond for phosphoproteins (bottom panel). The area and mean raw optical density (OD) of cMyBP-C and cTnI bands were determined and plotted against volume (μg) loaded. Regression lines were fitted to the data points and the resultant slope for proteins and phosphoproteins is shown in the top and bottom panel, respectively. Each data point represents the mean $\pm$ S.E.M.

the stretch activation response in endocardial fibres is significantly slower than epicardial fibres. Our results are also in agreement with a recent computational model by Campbell *et al.* (2008) which predicted that faster rates of cross-bridge kinetics as would occur with increased expression of α MHC in epicardial cells could explain the faster time course of cell shortening observed by Cordeiro *et al.* (2004). Thus, the kinetics of cross-bridge cycling in the myofilaments of ventricular myocytes is tuned to the calcium handling properties of the SR (Campbell *et al.* 2008) such that the contractile efficiency of the ventricle is maximized.

Physiological relevance of differential MHC expression on myocardial function

Several factors contribute to regional heterogeneity in fibre stretch and contraction during the cardiac cycle including ventricular fibre architecture, the transmural sequence of mechanical activation, and differences in the force generation capabilities of fibres across the ventricular wall. For instance, endocardial fibre shortening precedes that of epicardial fibre shortening; however, it has been observed (Sengupta *et al.* 2005; Ashikaga *et al.* 2007) that during isovolumic contraction, late activated epicardial fibres cause early activated endocardial fibres to become forcibly stretched (stretch activation) (Pringle, 1978). This occurs because endocardial fibres and epicardial fibres are arranged in opposing helical formations across the ventricular wall (Streeter *et al.* 1969), and because epicardial fibres generate more mechanical torque, in part, due to their longer radii and larger moment arms (Taber *et al.* 1996), which allows them to dominate

©2008 The Authors. Journal compilation © 2008 The Physiological Society

endocardial fibres during isovolumic contraction. Here we show that increased expression of the faster α MHC isoform in the epicardium serves to accelerate the rate of force development in epicardial fibres such that even though they are activated later than endocardial fibres, both shorten simultaneously during systolic ejection (Sengupta *et al.* 2006; Buckberg *et al.* 2006; Ashikaga *et al.* 2007). Conversely, decreased expression of α MHC in the endocardium acts to slow the rate of stretch-induced delayed force development so that the period of systolic ejection is prolonged, thereby enhancing the volume of blood ejected with each beat. Taken together, these data suggest that the transmural expression of MHC isoforms in porcine ventricle contributes to the timing of force generation across the ventricular midwall.

With the exception of MHC isoform expression, no differences in the relative abundance or phosphorylation status of other myofilament proteins were detected across the ventricular midwall in this study. Interestingly, a transmural gradient of RLC phosphorylation has been previously described in the left ventricle of mouse myocardium to account for the increased force production of the epicardium during the counterclockwise torsional twist of the ventricle at the time of ejection (Davis *et al.* 2001). The lack of difference in RLC phosphorylation in porcine endocardial and epicardial preparations in this study, however, may reflect a species difference between the mouse and the pig or the fact that our cardiac preparations were isolated from hearts under basal contractile states and therefore did not exhibit elevated levels of RLC phosphorylation in the epicardium, which have been reported to occur in isolated rat hearts during higher workloads (Hidalgo *et al.* 2006). It is also possible that the regional differences in RLC phosphorylation in porcine myocardium manifest themselves in a longitudinal plane (from apex to base) as has been reported in the rat heart (Rajashree *et al.* 2005), and thus, would not be evident by a cross-sectional analysis of the midwall alone.

In a similar fashion to isovolumic contraction, isovolumic relaxation in the heart is not a passive process, but rather involves significant regional heterogeneity in fibre shortening and lengthening (Ashikaga *et al.* 2004, 2007; Sengupta *et al.* 2006; Buckberg *et al.* 2006). In particular, endocardial fibre shortening has been observed to extend into the period of isovolumic relaxation after epicardial fibres have ceased to contract, resulting in stretch of the epicardial fibres (Ashikaga *et al.* 2004, 2007; Sengupta *et al.* 2006; Buckberg *et al.* 2006). This stretch during isovolumic relaxation has been proposed to contribute to the reversal of systolic torsional twist incurred by the left ventricle during systole, and therefore, acts to augment ventricular 'suction' so that diastolic filling is enhanced to provide for greater ejection of blood during the next beat (Torrent-Guasp *et al.* 2004). Consequently, stretch-induced delayed force development in the endocardium could be an important modulator of diastolic function by aiding in the reversal of systolic torsional twist during isovolumic relaxation.

Possible physiological implications of decreased α MHC expression in heart failure

Recent studies have suggested that the down-regulation of the α MHC isoform in chronic human heart failure contributes to diminished ventricular mechanical function (Lowes *et al.* 1997; Miyata *et al.* 2000; Reiser *et al.* 2001). While increased expression of the slower β MHC isoform in the heart reduces ATP utilization (Hoyer *et al.* 2007) and improves contractile efficiency (Narolska *et al.* 2005; Rundell *et al.* 2005), mechanical function is severely compromised at high workloads when

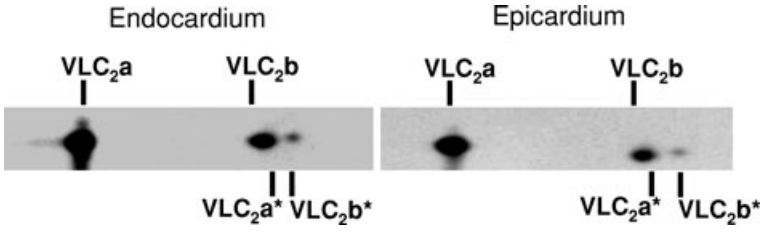

Figure 6. Myosin regulatory light chain (RLC) phosphorylation of porcine skinned myocardium
Two-dimensional SDS-PAGE/IEF gels were used to determine levels of RLC phosphorylation in endocardial (left panel) and epicardial (right panel) midwall skinned myocardium. In this representative gel two isoforms of ventricular light chain (VLC_2a and VLC_2b) and their corresponding phosphorylated isoforms (VLC_2a^* and VLC_2b^*) can be detected. It can be seen that VLC_2b and VLC_2a^* co-migrate similarly and are not readily separated; however, densitometric scans of the RLC spots in gels from four porcine hearts indicated that phosphorylation levels were not significantly different between endocardial and epicardial myocardium with VLC_2a^* and VLC_2b^* representing $13.5 \pm 3.1\%$ and $16.8 \pm 3.3\%$ of the total VLC_2a and VLC_2b content in the endocardium and epicardium, respectively.

©2008 The Authors. Journal compilation © 2008 The Physiological Society

pump function can not keep up with circulatory demands (Krenz & Robbins, 2004). Furthermore, therapies such as beta-adrenergic blockade (Lowes *et al.* 2002) or cardiac resynchronization (Iyengar *et al.* 2007) that reverse the loss of α MHC in heart failure patients have been found to improve contractile function, suggesting that decreased expression of α MHC is detrimental to normal cardiac function. Data from the present study show that a relatively small difference in MHC isoform content can dramatically affect myofilament contractile function as demonstrated by the acceleration in the kinetics of stretch activation and cross-bridge cycling in epicardial fibres *versus* endocardial fibres, presumably due to the ∼10% higher expression of α MHC isoform in epicardial fibres. Unlike the rodent cardiac α MHC isoform, which displays ∼2- to 3-fold faster rates of ATPase and force development compared with β MHC (Fitzsimons *et al.* 1998; Narolska *et al.* 2005; Stelzer *et al.* 2007), the cardiac α MHC isoform in human hearts (Narolska *et al.* 2005) displays significantly faster rates of ATPase and force development compared with the β MHC isoform. Thus, the loss of α MHC isoform in failing human hearts, though relatively small in absolute terms, can significantly slow the rate of force development in the ventricle, and thereby depress systolic ejection.

Another important factor which could affect the functional impact of loss of α MHC in failing myocardium is the region of the heart from which down-regulation occurs. Since MHC isoforms are differentially expressed across the ventricular wall, it is likely that a decrease in α MHC isoform expression in a region that normally expresses higher levels can have a profound functional effect. For example, a down-regulation of α MHC isoform in the epicardium would delay the onset of mechanical contraction and slow the rate of cross-bridge cycling such that stretch of endocardial fibres by epicardial fibres would be delayed. The resulting stretch activation response of endocardial fibres would then occur too late into the systolic phase to significantly contribute to ventricular ejection, thereby diminishing stroke volume and work production.

In summary, efficient myocardial pump function is dependent on the precise coordination and timing of regional mechanical activation (Markhasin *et al.* 2003), the loss of which significantly impairs systolic and diastolic function (Kass *et al.* 1999; Nelson *et al.* 2000; Cazeau *et al.* 2001; Sengupta *et al.* 2005, 2006). Here we show that the transmural distribution of MHC isoforms in porcine ventricle plays an important role in modulating the timing of force generation across the ventricular wall. Increased expression of α MHC in the epicardium accelerates the rate of force development such that shortening of the earlier-activated endocardial fibres are well coordinated with subsequently activated epicardial fibres during systolic ejection. Decreased expression of α MHC in the endocardium slows the rate of stretch-induced delayed force generation and serves to prolong the period of systolic ejection while maintaining the shortening of endocardial fibre during isovolumic relaxation to enhance diastolic filling via stretched epicardial fibres. Thus, the ventricular gradient of MHC isoforms in the heart contributes to mechanical function by fine-tuning the timing of force generation across the ventricular wall. Consequently, loss of α MHC during chronic human heart failure may disrupt the timing of mechanical contraction, and thereby, lead to compromised systolic and diastolic function.

References

Ashikaga H, Coppola BA, Hopenfeld B, Leifer ES, McVeigh ER & Omens JH (2007). Transmural dispersion of myofiber mechanics: implications for electrical heterogeneity *in vivo*. *J Am Coll Cardiol* **49**, 909–916.

Ashikaga H, Omens JH, Ingels NB Jr & Covell JW (2004). Transmural mechanics at left ventricular epical pacing site. *Am J Physiol Heart Circ Physiol* **286**, H2401–H2407.

Bogaert J & Rademakers FE (2001). Regional nonuniformity of normal adult human left ventricle. *Am J Physiol Heart Circ Physiol* **283**, H792–H799.

Bougaisky LB, Anderson PG, Hall RS & Bishop SP (1990). Differences in myosin isoform expression in the subepicardial and subendocardial myocardium during cardiac hypertrophy in the rat. *Circ Res* **66**, 1127–1132.

Bouvagnet P, Mairhofer H, Leger JO, Puech P & Leger JJ (1989). Distribution pattern of alpha and beta myosin in normal and diseased human ventricular myocardium. *Basic Res Cardiol* **84**, 91–102.

Brenner B & Eisenberg E (1986). Rate of force generation in muscle: correlation with actomyosin ATPase activity in solution. *Proc Natl Acad Sci U S A* **83**, 3542–3546.

Buckberg GD, Mahajan A, Jung B, Markl M, Hennig J & Ballester-Rodés M (2006). MRI myocardial motion and fiber tracking: a confirmation of knowledge from different imaging modalities. *Eur J Cardiothorac Surg* **29**, S165–S177.

Campbell KS & Moss RL (2003). SLControl: PC-based data acquisition and analysis for muscle mechanics. *Am J Physiol Heart Circ Physiol* **285**, H2857–H2864.

Campbell SG, Flaim SN, Leem CH & McCulloch AD (2008). Mechanisms of transmurally varying myocyte electromechanics in an integrated computational model. *Phil Trans R Soc A* **366**, 3361–3380.

Carnes CA, Geisbuhler TP & Reiser PJ (2004). Age-dependent changes in contraction and regional myocardial myosin heavy chain isoform expression in rats. *J Appl Physiol* **97**, 446–453.

Cazeau S, Leclercq C, Lavergne T, Walker S, Varma C, Linde C, Garrigue S, Kappeneberger L, Haywood GA, Santini M, Bailleul C & Daubert JC (2001). Effects of multisite biventricular pacing in patients with heart failure and intraventricular conduction delay. *N Engl J Med* **344**, 873–880.

©2008 The Authors. Journal compilation © 2008 The Physiological Society

Cazorla O, Szilagyi S, Le Guennec JY, Vassort G & Lacampagne A (2005). Transmural stretch-dependent regulation of contractile properties in rat heart and its alteration after myocardial infarction. *FASEB J* **19**, 88–90.

Cordeiro JM, Greene L, Heilmann C, Antzelevitch D & Antzelevitch C (2004). Transmural heterogeneity of calcium activity and mechanical function in the canine left ventricle. *Am J Physiol Heart Circ Physiol* **286**, H1471–H1479.

Davis JS, Hassanzadeh S, Winitsky S, Lin H, Satorius C, Vemuri R, Aletras AH, Wen H & Epstein ND (2001). The overall pattern of cardiac contraction depends on a spatial gradient of myosin regulatory light chain phosphorylation. *Cell* **107**, 631–641.

Diffee GM & Nagle DF (2003). Regional differences in effects of exercise training on contractile and biochemical properties of rat cardiac myocytes. *J App Physiol* **95**, 35–42.

Fabiato A (1988). Computer programs for calculating total from specified free or free from specified total ionic concentrations in aqueous solutions containing multiple metals and ligands. *Methods Enzymol* **157**, 378–417.

Fitzsimons DP, Patel JR, Campbell KS & Moss RL (2001). Cooperative mechanisms in the activation dependence of the rate of force development in rabbit skinned skeletal muscle fibers. *J Gen Physiol* **117**, 133–148.

Fitzsimons DP, Patel JR & Moss RL (1998). Role of myosin heavy chain composition in kinetics of force development and relaxation in rat myocardium. *J Physiol* **513**, 171–183.

Godt RE & Lindley BD (1982). Influence of temperature upon contractile activation and isometric force production in mechanically skinned muscle fibers of the frog. *J Gen Physiol* **80**, 279–297.

Hidalgo H, Wu Y, Peng J, Siems WF, Campbell KB & Granzier H (2006). Effect of diastolic pressure on MLC2v phosphorylation in the rat left ventricle. *Arch Biochem Biophys* **456**, 216–223.

Hoh JFY, Yeoh GPS, Thomas MAW & Higgenbottom L (1979). Structural differences in the heavy chains of rat ventricular myosin isoenzymes. *FEBS Lett* **97**, 330–334.

Hoyer K, Krenz M, Robbins J & Ingwall JS (2007). Shifts in the myosin heavy chain isozymes in the mouse heart result in increased energy efficiency. *J Mol Cell Cardiol* **42**, 214–221.

Iyengar S, Haas G, Lamba S, Orsinelli DA, Babu GJ, Ferketich AK, Yamokosi L, Periasamy M & Abraham WT (2007). Effect of cardiac resynchronization therapy on myocardial gene expression in patients with nonischemic dilated cardiomyopathy. *J Card Fail* **13**, 304–311.

Kass DA, Chen CH, Curry C, Talbot M, Berger R, Fetics B & Nevo E (1999). Improved left ventricular mechanics from acute VDD pacing in patients with dilated cardiomyopathy and ventricular conduction delay. *Circulation* **99**, 1567–1573.

Krenz M & Robbins J (2004). Impact of beta-myosin heavy expression on cardiac function during stress. *J Am Coll Cardiol* **44**, 2390–2397.

Kuro-o M, Tsuchimochi H, Ueda S, Takaku F & Yazaki Y (1986). Distribution of cardiac myosin isozymes in human conducation system. Immunohistochemical study using monoclonal antibodies. *J Clin Invest* **77**, 340–347.

Laurita KR, Katra R, Wible B, Wan X & Koo MH (2003). Transmural heterogeneity of calcium handling in canine. *Circ Res* **92**, 668–675.

Litten RZ, Martin BJ, Buchthal RH, Nagai R, Low RB & Alpert NR (1985). Heterogeneity of myosin isozyme content of rabbit heart. *Circ Res* **57**, 406–414.

Liu DW, Gintant GA & Antzelevitch C (1993). Ionic bases for electrophysiological distinctions among epicardial, midmyocardial, and endocardial myocytes form the free wall of the canine left ventricle. *Circ Res* **72**, 671–687.

Lowes BD, Gilbert EM, Abraham WT, Minobe W, Larrabee P, Ferguson D, Wolfel EE, Lindenfeld J, Tsvetkova T, Robertson AD, Quaife RA & Bristow MR (2002). Myocardial gene expression in dilated cardiomyopathy treated with beta-blocking agents. *N Engl J Med* **346**, 1357–1365.

Lowes BD, Minobe W, Abraham T, Rizeq MN, Bohlmeyer TJ, Quaife RA, Roden RL, Dutcher DL, Robertson AD, Voelkel NF, Badesch DB, Groves BM, Gilbert EM & Bristow MR (1997). Changes in gene expression in the intact human heart: downregulation of a-myosin heavy chain in hypertrophied, failing ventricular myocardium. *J Clin Invest* **100**, 2315–2324.

McDonald KS, Mammen PPA, Strang KT, Moss RL & Miller WP (1995). Isometric and dynamic contractile properties of porcine skinned cardiac myocytes after stunning. *Circ Res* **77**, 964–972.

Markhasin VS, Solovyova O, Katsnelson LB, Protsenko Y, Kohl P & Noble D (2003). Mechano-electric interactions in heterogeneous myocardium: development of fundamental experimental and theoretical models. *Prog Biophys Mol Biol* **82**, 207–220.

Miyata S, Minobe W, Bristow MR & Leinwand LA (2000). Myosin heavy chain isoform expression in the failing and nonfailing human heart. *Circ Res* **86**, 386–390.

Narolska NA, van Loon RB, Boontje NM, Zaremba R, Penas SE, Russell J, Spiegelenberg SR, Huybregts MA, Visser FC, de Jong JW, van der Velden J & Stienen GJM (2005). Myocardial contraction is 5-fold more economical in ventricular than atrial tissue. *Cardiovasc Res* **65**, 221–229.

Nelson GS, Curry CW, Wyman BT, Kramer A, Declerck J, Talbot M, Douglas MR, Berger RD, McVeigh ER & Kass DA (2000). Predictors of systolic augmentation from left ventricular preexcitation in patients with dilated cardiomyopathy and intarventricular conduction delay. *Circulation* **101**, 2703–2709.

Pringle JWS (1978). The Croonian Lecture, 1977. Stretch activation of muscle: function and mechanism.*Proc R Soc Lond B Biol Sci* **201**, 107–130.

Rajashree R, Blunt BC & Hofmann PA (2005). Modulation of myosin phosphatase targeting subunit and protein phosphatase 1 in the heart. *Am J Physiol Heart Circ Physiol* **289**, H1736–H1743.

Reiser PJ, Portman MA, Ning XH & Moravec CS (2001). Human cardiac myosin heavy chain isoforms in fetal and failing adult atria and ventricles. *Am J Physiol Heart Circ Physiol* **280**, H1814–H1820.

Rundell VL, Manaves MV, Martin AF & deTombe PP (2005). Impact of b-myosin heavy chain isoform expression on cross-bridge cycling kinetics. *Am J Physiol Heart Circ Physiol* **288**, H896–H903.

Schevchenko A, Wilm M, Vorm O & Mann M (1996). Mass Spectrometric sequencing of proteins from silver-stained polyacrylamide gels. *Anal Chem* **68**, 850–858.

©2008 The Authors. Journal compilation © 2008 The Physiological Society

Schiaffino S & Reggiani C (1996). Molecular diversity of myofibrillar proteins: gene regulation and functional significance. *Physiol Rev* **76**, 371–423.

Sengupta PP, Khandheria BK, Korinek J, Wang J & Belohlavek M (2005). Biphasic tissue Doppler waveforms during isovolumic phases are associated with asynchronous deformation of subendocardial and subepicardial layers. *J Appl Physiol* **99**, 1104–1111.

Sengupta PP, Korinek J, Belohlavek M, Narula J, Vannan MA, Jahangir A & Khandheria BK (2006). Left ventricular structure and function: basic science for cardiac imaging. *J Am Coll Cardiol* **48**, 1988–2001.

Stelzer JE, Brickson SL, Locher MR & Moss RL (2007). Role of myosin heavy chain in the stretch activation response of rat myocardium.*J Physiol* **579**, 161–173.

Stelzer JE, Fitzsimons DP & Moss RL (2006*a*). Ablation of myosin binding protein-C accelerates force development in mouse myocardium. *Biophys J* **90**, 4119–4127.

Stelzer JE, Larsson L, Fitzsimons DP & Moss RL (2006*b*). Activation dependence of stretch activation in mouse skinned myocardium: implications for ventricular function. *J Gen Physiol* **127**, 95–107.

Stelzer JE, Patel JR & Moss RL (2006*c*). PKA-mediated acceleration of the stretch activation response in myocardium is eliminated by ablation of cMyBP-C. *Circ Res* **99**, 884–890.

Stelzer JE, Patel JR & Moss RL (2006*d*). Acceleration of stretch activation in murine myocardium due to phosphorylation of myosin regulatory light chain. *J Gen Physiol* **128**, 261–272.

Streeter DD Jr, Spotnitz HM, Patel DP, Ross J Jr & Sonnenblick EH (1969). Fiber orientation in the canine left ventricle during diastole and systole. *Circ Res* **24**, 339–347.

Taber LA, Yang M & Podszus WW (1996). Mechanics of ventricular torsion. *J Biomech* **29**, 745–752.

Torrent-Guasp F, Kocica MJ, Corno A, Komeda M, Cox J, Flotats A, Ballester-Rodés M & Carreras-Costa F (2004). Systolic ventricular filling. *Eur J Cardiothorac Surg* **25**, 376–386.

Warren CM & Greaser ML (2003). Method for cardiac myosin heavy chain separation by sodium dodecyl sulfate gel electrophoresis. *Anal Biochem* **320**, 149–151.

Acknowledgements

This study was supported by National Institutes of Health grant HL61635 (R.L.M.).

©2008 The Authors. Journal compilation © 2008 The Physiological Society